ICES Journal of Marine Science, 56: 545–560. 1999
Article No. jmsc.1999.0480, available online at http://www.idealibrary.com on IDEAL®

Spatial proximity of age-0 walleye pollock (*Theragra chalcogramma*) to zooplankton near the Pribilof Islands, Bering Sea, Alaska

G. Swartzman, R. Brodeur, J. Napp, G. Hunt, D. Demer, and R. Hewitt

Swartzman, G., Brodeur, R., Napp, J., Hunt, G., Demer, D., and Hewitt, R. 1999. Spatial proximity of age-0 walleye pollock (*Theragra chalcogramma*) to zooplankton near the Pribilof Islands, Bering Sea, Alaska. – ICES Journal of Marine Science, 56: 545–560.

Acoustic surveys, conducted in September 1994 and 1995 in the neighbourhood of the Pribilof Islands, Alaska, collected data at three frequencies, making possible the location of pollock shoals and patches of zooplankton along the survey transect. These patches were identified using threshold and morphological filters on echosounder images taken at 38 kHz (fish identification) and 120 and 200 kHz (plankton identification). We checked the morphological methods by comparing the depth distribution of acoustically determined plankton with zooplankton from net surveys and found them in general agreement. Our ability to spatially map patches of plankton and shoals of fish (mostly pollock) along the survey transects led to our examining the spatial proximity between pollock and plankton patches. Results, using both interval- and distance-based measures, suggested that fish–plankton proximity was affected by plankton biomass. When the plankton biomass was low, fish tended to remain close to existing plankton patches, while at high plankton biomass there was no consistent small-scale proximity relationship. At intermediate plankton densities there was no particular distance-based proximity of plankton patches to fish shoals. However, the interval-based fish densities tended to increase with increasing plankton density up to some plankton density threshold, above which there was no clear association between fish and plankton density. These findings suggest the existence of plankton biomass density thresholds, both overall and within plankton patches that may influence pollock feeding strategies. They also suggest a possible method for empirically estimating these thresholds using multi-frequency acoustic survey data.

Key words: acoustics, walleye pollock, zooplankton patchiness, predator–prey relationships, Generalized Additive models, distance-based proximity.

Received 24 June 1998; accepted 5 April 1999.

G. Swartzman: Applied Physics Laboratory and School of Fisheries, University of Washington, Seattle, WA 98105, USA. R. Brodeur and J. Napp: Alaska Fisheries Science Center, National Marine Fisheries Service, Seattle WA 7600 Sand Point Way N.E., Seattle, WA 98115, USA. G. Hunt: Department of Evolutionary Biology, University of California, Irvine, CA 92697, USA. D. Demer and R. Hewitt: Southwest Fisheries Science Center, National Marine Fisheries Service, La Jolla, CA 92073, USA. Correspondence to G. Swartzman: tel: +1 206 543 0061; fax: +1 206 543 6785; e-mail: gordie@apl.washington.edu

Introduction

The Pribilof Islands are an important juvenile walleye pollock (*Theragra chalcogramma*) nursery area. They are also a major breeding area for birds and marine mammals, including piscivorous murres (*Uria* spp.), puffins (*Fratercula* spp.), and northern fur seals (*Callorhinus ursinus*), all of which prey on juvenile pollock (Coyle *et al.*, 1992; Springer, 1992; Decker and Hunt, 1996). Due to the importance of pollock as a forage fish, as a plankton consumer, and as the basis for a huge commercial fishery, the determinants of year-class strength for this nodal species deserve close scrutiny.

1054–3139/99/040545+16 $30.00/0

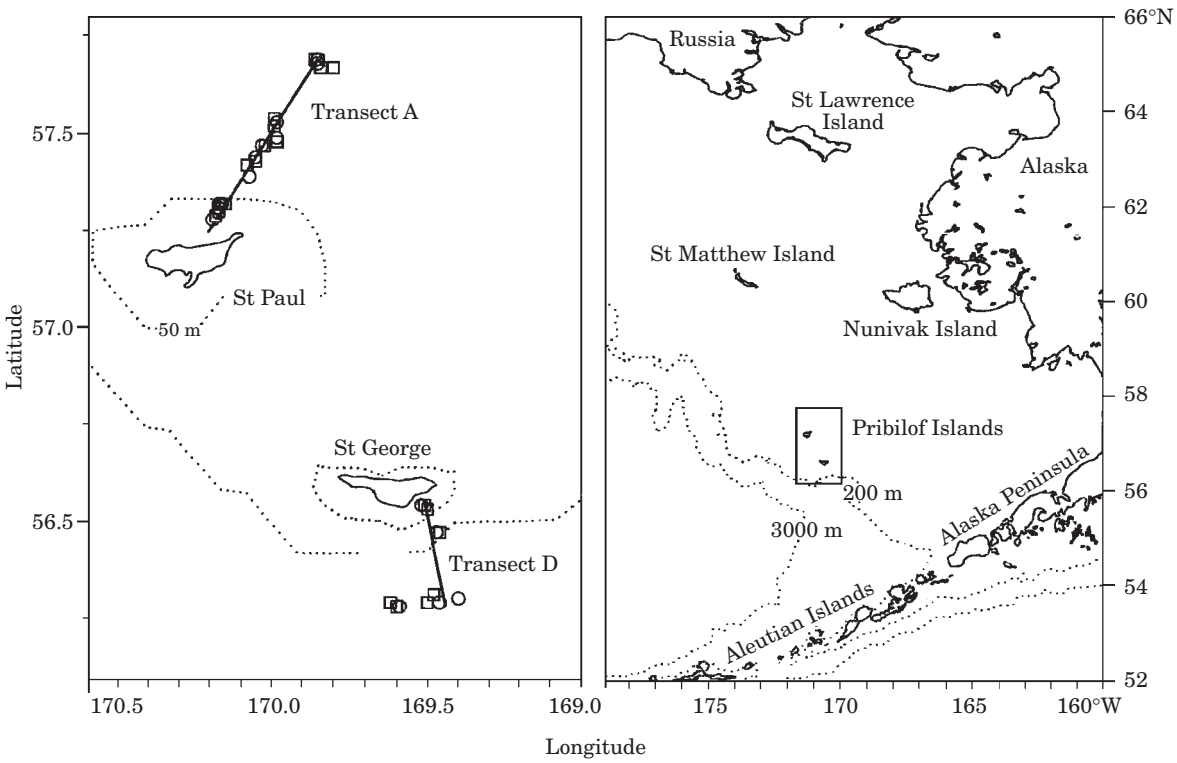

Figure 1. Pribilof Island study region in the eastern Bering Sea showing locations of the A and D transect lines. Locations of MOCNESS hauls (squares) and Methot trawls (circles) along the transects are shown as well as the 50 and 100 m isobaths.

A series of acoustic surveys, conducted by the National Marine Fisheries Service (NMFS) as part of the Bering Sea Fisheries Oceanography Coordinated Investigations (BSFOCI) programme in September 1994 and 1995, offer a unique opportunity to examine the spatial proximity of juvenile pollock and their prey (primarily copepods and euphausiids, but also, for larger juveniles, other pollock). Although close proximity to their prey is not the only determinant of pollock feeding and survival, we see examining pollock–plankton spatial relationships as a first step to developing an improved understanding of the role of prey availability in pollock year-class strength. Therefore, we are interested in developing means of measuring and testing for proximity of pollock and their prey.

Measurements of environmental conditions (salinity and temperature) allowed identification of hydrographic features along the survey track and provided an environmental context for examination of predator–prey proximity (Brodeur *et al.*, 1997). The study transects radiated from the Pribilof Islands and crossed frontal boundaries (Figure 1). Thus, the transects could be characterized as divided into separate, front-delineated water masses – a well-mixed nearshore region, a stratified offshore region, and a front or transition region between them. These regions provided convenient subdivisions for a study of fish and zooplankton (also referred to hereafter as plankton) distributions because, as we will show here, the degree of stratification plays a major role in the diel vertical migration pattern of fish and plankton and its effect on their proximity to each other.

Algorithms for identification of fish shoals and plankton patches from these acoustic data form the basis for this study. This paper focuses on survey data from 1994 and 1995. In this paper, we also discuss evidence in support of the success of our plankton identification algorithm.

Focal questions

This paper is organized around four questions: How the spatial distributions of pollock and plankton change from year-to-year, transect to transect and day to night?; How does the spatial distribution of age-0 pollock relate to that of their zooplankton prey?; Are there consistent differences in predator–prey proximity and biomass between the transects that hold over years, and, if so, are these differences related to differences in frontal structure and current patterns around the Pribilof Islands?; Are differences in the proximity between pollock and their prey related to differences in their relative abundance?

Methods

Acoustic surveys were conducted in mid-September 1994, and 1995 aboard the NOAA ships "Miller Freeman" and "Surveyor". Vertical profiles of temperature and salinity were obtained from 8–10 CTD casts along each transect (Stabeno *et al.*, 1998). Here, data is included from Transect A, northeast of St Paul Island, and Transect D, southeast of St George Island (Figure 1). These transects were chosen because they had the most clearly defined hydrographic regions, were the most frequently sampled, and had the most complete set of ancillary biological and environmental data.

Acoustic data were collected using SIMRAD EK500 echosounder systems, centerboard- and hull-mounted, respectively, on the two vessels, and recording at 38 ("Miller Freeman"), 120 (both vessels), and 200 ("Surveyor") kHz. The ping data were subsampled to provide backscatter images of 1000 pixels horizontal per 8 km, with 0.5 m vertical resolution. All transducers were calibrated prior to each cruise by the standard sphere method (Foote *et al.*, 1987).

Fish species and size composition were sampled both on targets and at preselected locations along the transects using anchovy and Methot trawls (Brodeur *et al.*, 1997). Meso-zooplankton depth distributions and species composition were obtained using a 1 m^2 MOCNESS (Multiple Opening/Closing Net and Environmental Sampling System; Wiebe *et al.*, 1976) with a 333 μm mesh net. Macrozooplankton captured and retained by the Methot trawl (2 × 3 mm mesh liner) were also enumerated. Additionally, juvenile pollock samples were taken to determine diet and condition by year and hydrographic region (Brodeur *et al.*, 1997).

This study does not provide detailed catch composition for these sampling devices because they are available elsewhere (Brodeur *et al.*, 1997; Brodeur, 1998). Both the anchovy and Methot trawls caught predominately age-0 walleye pollock (>95% catch by number) and large medusae, whereas the MOCNESS caught mainly euphausiids, chaetognaths, and copepods.

Patch identification and description

Acoustic data images (1000 × 500 pixels) were "cleaned" using bottom and near-surface bubble layer cleaning algorithms (Swartzman *et al.*, 1994). The images were combined into a continuous image for each transect for inclusion in a new, multi-purpose data viewer (Swartzman *et al.*, 1999).

Fish shoals were identified using the 38 kHz echosounder images. A lower threshold filter of − 53 dB was applied to the cleaned images. This eliminates all pixels with lower backscatter, leaving only pixels expected to be in the range of backscatter target strength for the size range of pollock sampled (− 37 to − 53 dB; Traynor, 1996; Brodeur and Wilson, 1996). A morphological image processing binary filter with a 3 × 2 pixel (horizontal by vertical) structuring element was then applied using a closing followed by an opening operation (Haralick and Shapiro, 1992). The 3 × 2 pixel structuring element is large enough such that, with the morphological filters used, small targets (e.g. individual fish) were eliminated, leaving only fish shoals. This filtered image was then multiplied by the original image, producing an image with only identified shoals, but with pixel values from the original image, thereby assuring no alteration in average volume backscatter (S_V) or in backscatter variance within the shoals. In summary, the morphological method relies on three aspects expected for shoaling fish: (1) S_V in the range of − 37 to − 53 dB; (2) contiguous pixels having S_V in this range; and (3) a well-recognized boundary along which S_V declines from the expected range for fish to levels below this range (Swartzman *et al.*, 1994).

Plankton patches were identified using spatially-matched acoustic echograms at 120 and 200 kHz. In this algorithm plankton were not distinguished by taxonomic or functional group, but included all scatterers within a size range acoustically detectable at the survey frequencies. After bottom and bubble layer cleaning, we applied a background threshold filter between − 74 and − 54 dB to the echograms, which set all pixels outside this range to the background level. The − 74 to − 54 dB range was chosen to represent a range of S_V expected for patches of zooplankton, especially euphausiids and large copepods. Volume backscatter[1] is the sum of the individual target strengths (incorporating the effects of cross-sectional area, orientation, and sound speed and density contrast between the organisms and the surrounding water) weighted by the concentration of each scatterer type (Stanton *et al.*, 1993). The 120 kHz echogram S_V was then subtracted from that of the 200 kHz echogram and a +2 dB foreground threshold was applied to the resulting image (i.e. all pixels in the 200 kHz echogram having S_V less than 2 dB greater than the 120 kHz echogram were set to 0). The implicit assumption is that Rayleigh, rather than geometric scattering dominates the S_V for these organisms at 120 and 200 kHz. Geometric computations using a bent cylinder model for euphausiids (Stanton *et al.*, 1993) and a truncated sphere model for copepods (Holliday and Pieper, 1995) in the size range found in the MOCNESS samples suggest that this assumption is valid for the dominant zooplankton in this area.

Plankton patches were delineated on the resulting image using a binary morphological filter with a 3 × 2

[1]Backscatter and S_V are used interchangeably throughout this paper. The units are in dB. However, backscatter may also be in power units (volts). In this case we refer to the backscatter as s_V. The transformation between them is standard (Urick, 1983).

Table 1. Attributes of shoals and patches saved for statistical analysis by the connected component algorithm.

Attribute type	Attribute
Location	Latitude, longitude (degrees, decimal minutes), depth
Size	Height (m), width (m), area (m^2), octuples of latitude and longitude delineating the polygon edge of each aggregation (degrees, decimal minutes)
Backscatter	Average s_v (volts), mean S_v (dB)

pixel sphere closing followed by an opening. This binary image was then multiplied by the original 200 kHz image, leaving an image having all non-background pixels associated with patches and having their original 200 kHz S_V values. This algorithm uses several expected features of plankton patches: (1) S_V in the range of -74 to -54 dB; (2) contiguous pixels having backscatter in this range; (3) backscatter within the patch more than 2 dB higher at 200 kHz than at 120 kHz; and (4) the patch is a clearly defined entity with a clear boundary beyond which backscatter is outside the expected range. By using the 2 dB rule we expected to eliminate all scatterers (e.g. fish and medusae), which, although in the currect backscatter range, do not have higher backscatter at the higher frequency.

We used a connected component algorithm (Haralick and Shapiro, 1992) on the images after patch identification to produce a fish shoal or plankton patch table consisting of attributes of the shoals or patches (Table 1; Nero and Magnuson, 1989. The patch attributes provided a parsimonious description of the location, size, and shape of each fish shoal and plankton patch).

The transects (A and D) were divided into three regions; a nearshore well-mixed region (very small for Transect D due to the steep topography near St George Island), an offshore stratified region and a partially stratified front or transition region. On Transect D the middle region is more appropriately termed a slope region because it was completely stratified, but is shallower than the offshore region. The boundary between offshore and front regions for Transect A was defined by comparing the depth range of the thermocline between adjacent CTD casts. The offshore region included all CTD stations in which the depth range of the thermocline was less than or equal to twice the depth range for the clearly stratified CTD stations (Stabeno *et al.*, 1998). The boundary between the front and nearshore region was set to the deepest CTD station where the temperature range over depth was less than 2°C, as expected in a completely mixed region.

Proximity analysis

For each transect run in 1994 and 1995 the fish shoal and plankton patch data were divided into the three regions discussed above. Proximity was investigated within each of these regions using two methods. The first involved modelling fish shoal biomass[2] (shoal area × average shoal s_V) as a function of a plankton patch biomass (patch area × average patch s_V) using non-parametric Generalized Additive models (GAM; Hastie and Tibshirani, 1990). Alternatively, GAM was used to model density of fish in the shoal (average shoal s_V) as a function of plankton patch density (average patch s_V). The second set of GAMs was run to explore whether higher density fish shoals (higher average s_V) were spatially associated with higher density plankton patches. For the GAM model the fish and zooplankton biomass were apportioned into equal sized bins ranging in length from 100 m to 1 km. We used 100, 250, 500, and 1000 m bins, though only results for the 250 m bins are reported here. Results were not sensitive to bin size over the chosen range.

An alternative distance-based measure of proximity (Swartzman *et al.*, 1999) plotted the distribution of the plankton biomass as a function of distance h from each fish shoal. Each shoal was treated as a rectangle, although the method is applicable to any arbitrary shaped polygon (Swartzman *et al.*, 1999). Distance h is the horizontal distance from the edges of the rectangle. The biomass measure at any distance h is the sum of the biomass of all plankton patches included within a rectangle extending h metres from both ends of a fish shoal. This computation was made for each fish shoal and then the average over all fish shoals was plotted, for a range of distances h from 0 to 1 km, in increments of 100 m. This empirical proximity measure was then compared with a simulated random distribution of plankton patches by Monte Carlo sampling of the patches a large number of times (e.g. n=100) with patch centres randomly distributed over the region of interest. The proximity measure was recomputed for each random shuffling of patches (the sizes of the patches were not changed). Departure from randomness occurred when the empirical proximity measure was outside the range of proximity measures calculated for 95% of the reshuffled patches (for a 95% confidence limit).

The proximity measure provided both a test for randomness and an indication of the distance range over

[2]The term *biomass* is used generically here to refer to an index of biomass, which has not been corrected for the size, target strength, or density of organisms. Comparison between years and between regions which use the same biomass index assume a comparison of similar-sized organisms. The term *shoal* is used for fish to denote an aggregation or layer of fish that are not necessarily swimming in a polarized fashion. The more general term *patch* is used to denote plankton aggregations. It could also be applied to fish aggregations.

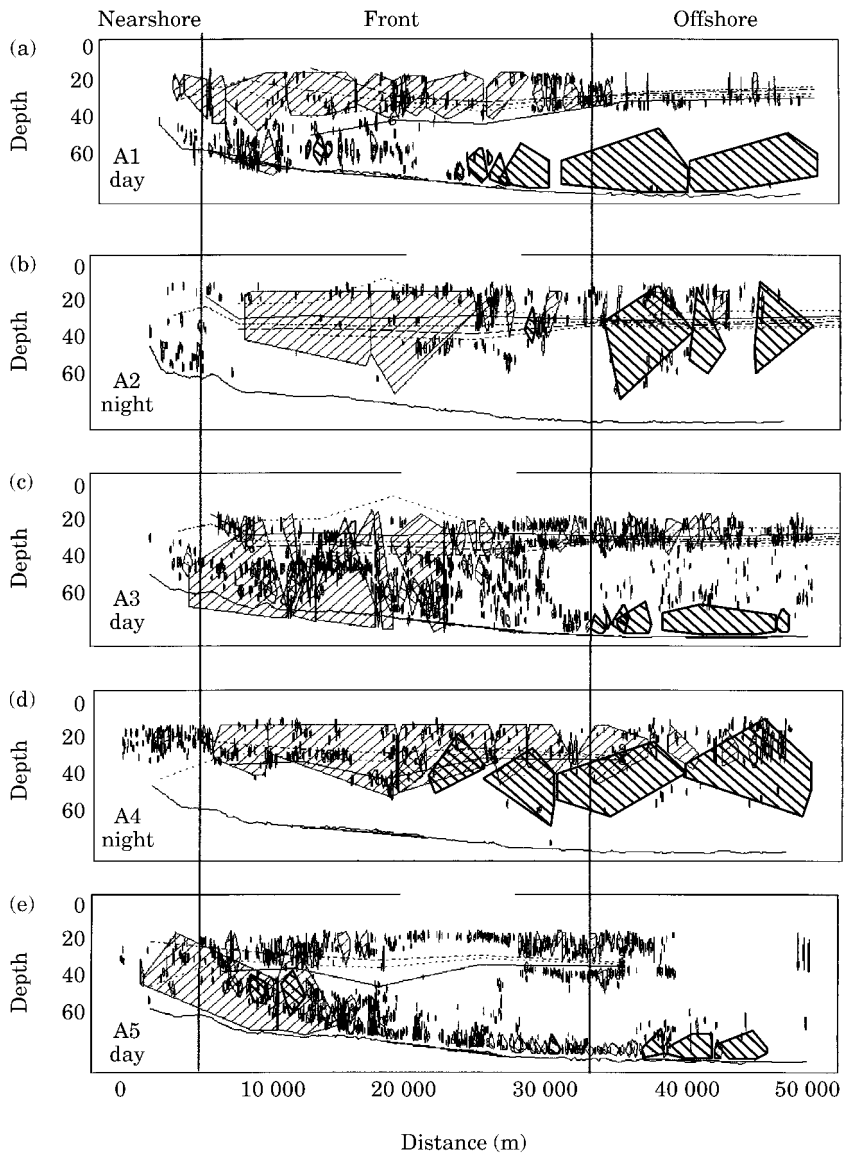

Figure 2. Distribution of plankton and fish with environmental data for five runs of Transect A in September 1995. Isotherms are shown based on CTD data. Fish (▨) and plankton (▧) polygons show the extent of the patches over three regions. The bottom is shown by a solid line on each panel.

which non-random patch distributions occurred (i.e. possible indications of clustering or inhibition of plankton patches around fish shoals). The biomass proximity method is similar to Ripley's K in spatial statistics (Diggle, 1983). It has the advantage over the GAM method and other bin-specific methods (e.g. spectral analysis) that it does not require horizontal overlap between fish and plankton to show proximity. During the day, plankton and fish were vertically separated. However, when vertical current shear is low, daytime horizontal overlap is not necessary to allow effective contact at night (i.e. the fish could be within some proximate access distance from the plankton during the daytime).

Results

Exploratory analysis

Transect A and D fish shoals and plankton patches were plotted as polygons (octagons) which show the convex hull (bounding polygon) for each separate patch and shoal as hatched polygons (Figures 2 and 3 for transect A and Figures 4 and 5 for transect D, 1995 and 1994,

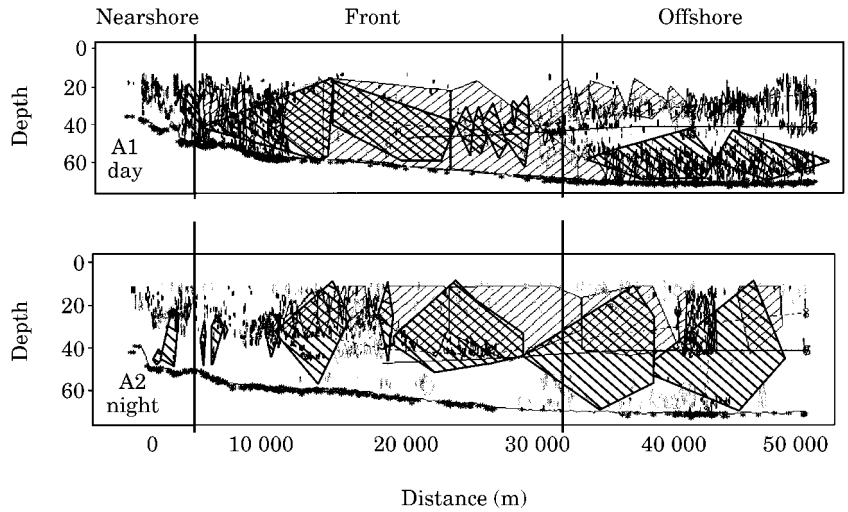

Figure 3. Distribution of plankton and fish with environmental data for two runs of Transect A in September 1994. Polygons for fish (▨) and plankton (▧) are shown over three hydrographic regions, with isotherms based on CTD data.

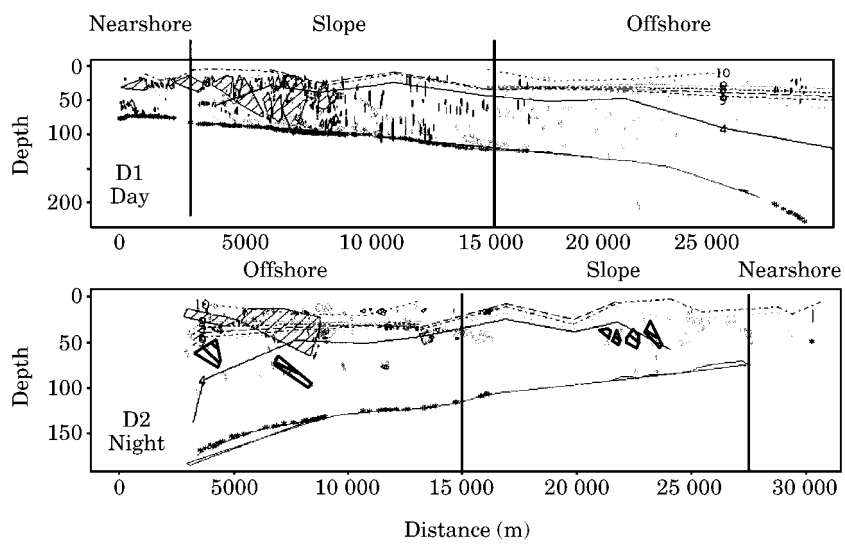

Figure 4. Distribution of plankton and fish with environmental data for two runs of Transect D in September 1995. Polygons for fish (▨) and plankton (▧) are shown over three depth regions, with isotherms based on CTD data and bottom.

respectively). Isotherms and bottom locations are overlaid on the images. For both years and transects, juvenile pollock tended to remain above (or close to) the thermocline both day and night, especially in the offshore region. Whenever large fish shoals were identified below the thermocline (Figures 2c, e and 3a) they consisted of larger, adult fish (identified as such by individual fish target strengths in the neighbourhood of the shoals). Diel migration of plankton is apparent, especially in the offshore, stratified region, with plankton being close to the bottom during the day and rising up in the water column to just below and into the pollock layer during night-time. The thermocline in 1995 was shallower than in 1994 for both transects (about 40 m in 1994 and 25 m in 1995; compare Figures 2 and 3). Thus, the pollock tended to be higher in the water column in 1995 than in 1994. This resulted in thicker (greater depth range) pollock shoals in 1994 than in 1995. Nearshore regions had smaller plankton patches and fish shoals. For Transect A, the offshore region tended to have larger plankton patches than the front region. The front region tended to have larger pollock shoals which were less restricted to above the thermocline than the offshore region (i.e. there were more adult

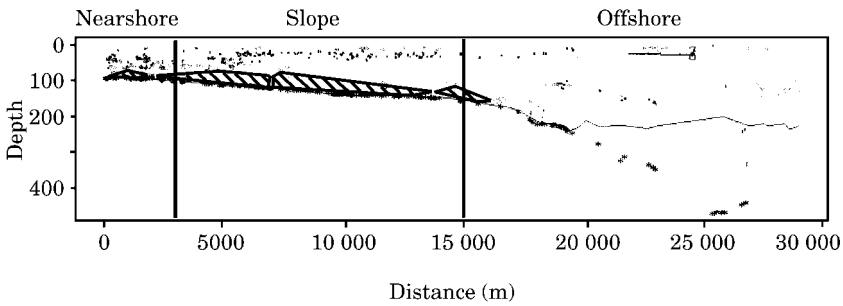

Figure 5. Transect D, daytime, September 1994 locations of fish shoals (▨) and plankton patches (▧) over three depth-delineated regions.

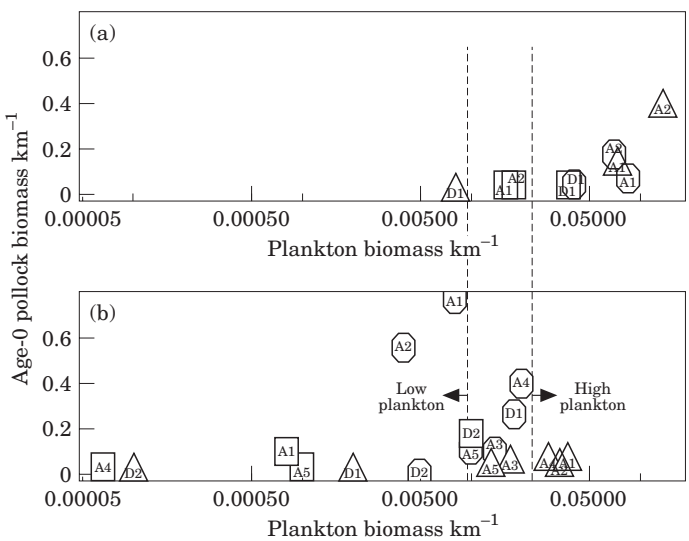

Figure 6. Plot showing density (biomass km^{-1}) for pollock and plankton for (a) 1994 and (b) 1995 with regions of low, medium, and high plankton densities. □, nearshore; ○, slope and front; △, offshore.

pollock in this region). For Transect D, most of the plankton and pollock tended to be in the slope region (Figures 4 and 5), although one transect run (Figure 4b) showed higher pollock biomass in the offshore region.

Transect A had pervasive pollock shoals both day and night in both 1994 and 1995, with extremely large plankton patches (up to 20 km in extent) blanketing the offshore region and extending in 1994 (and sometimes in 1995) into the front region as well. Transect D, a region dominated by advective flow along the shelf edge and thus considerably more hydrologically variable than Transect A (Stabeno *et al.*, 1998), had extensive plankton patches in the slope region in 1994, but considerably smaller and less pervasive patches in 1995 (Figures 4 and 5). The spatial extent of both pollock shoals and plankton patches is remarkable in both years and the areal coverage of the transected region by plankton patches and fish shoals was a considerable fraction of the total area transected. Therefore, our measure of proximity based on distance between predator and prey patches considers the spatial extent of the patches themselves.

Distribution of biomass

Fish densities along Transect A were similar for both years, however, the biomass km^{-1} shifted from being highest in the offshore region in 1994 to highest in the frontal region in 1995. Plankton biomass km^{-1} was, on average, higher offshore than in the frontal region for both years and was considerably higher in 1994 than in 1995 (Figure 6).

Fish biomass km^{-1} along Transect D was quite variable in 1995 (there was only a single transect run in 1994 so variability was not measurable) suggesting that the advection-dominated hydrography in this region may result in considerable movement of fish over short time periods. Plankton densities, as on Transect A, were higher in 1994 than 1995, suggesting that feeding

Table 2. Results of Generalized Additive models and distance-based proximity tests between fish and plankton for Transects A and D 1994 and 1995.

Year	Transect	Region	Within patch s_v test p value	Total biomass test p value	Distance-based proximity
1994	A1-day	Nearshore	—	—	Random
		Frontal	n.s.	0.003	Clustered
		Offshore	0.003	n.s.	Clustered
1994	A2-night	Nearshore	—	—	Clustered
		Frontal	n.s.	n.s.	Clustered
		Offshore	0.0002	n.s.	Inhibition to 500 m
1994	D1-day	Nearshore	—	—	Clustered to 400 m
		Slope	n.s.	0.241	Random
		Offshore	n.s.	n.s.	Clustered
1995	A1-day	Nearshore	—	—	Random
		Frontal	n.s.	n.s.	Inhibition
		Offshore	n.s.	n.s.	Random
1995	A2-night	Frontal	n.s.	n.s.	Clustered >200 m; inhibition at 0 m
1995	A2-night	Offshore	0.005	0.045	Inhibition
1995	A3-day	Offshore	0.001	0.114	Random
		Offshore	0	n.s.	Clustered <200 m
1995	A4-night	Nearshore	—	—	Clustered
		Frontal	n.s.	0.162	Inhibition
		Offshore	0.09	0.242	Inhibition
1995	A5-day	Nearshore	—	—	Clustered
		Frontal	0.001	n.s.	Clustered
		Offshore	0.0009	0.001	Clustered at 0 m
1995	D1-day	Slope	0.072	0.002	Random
		Offshore	n.s.	n.s.	Clustered
1995	D2-night	Nearshore	n.s.	n.s.	Clustered
		Slope	0	0	Clustered
		Offshore	n.s.	n.s.	Clustered

n.s. denotes not significant. — denotes that there were insufficient data in that region to perform the test.

conditions throughout the Pribilof Island area may have been better in 1994 than in 1995.

Proximity

Results for the GAM biomass and density overlap tests with a 250 m bin interval, as well as the distance-based biomass-proximity index are given in Table 2.

In regions having low plankton biomass (i.e. biomass km^{-1} <0.01) the distance-based proximity test tended to have plankton patches not randomly distributed around fish shoals, but rather clustered, while in regions with high plankton biomass (biomass km^{-1} >0.025) the spatial proximity was mixed. The lowest Transect A plankton biomass occurred in 1995 in the frontal region for A1, A2, and A5 and in the nearshore region for all runs (Figure 6). Transect D had low plankton densities offshore for both years (except run D2) and in the slope and nearshore regions for D2 in 1995. Among these low plankton density regions 9 of 11 had plankton patches being closer to fish shoals than would be expected in a random distribution of the plankton around the shoals (i.e. clustered in the proximity test; Table 2).

The high plankton density regions included the frontal and offshore regions of Transect A in 1994, the offshore region of A1, A2, and A4 in 1995 and the slope and nearshore regions of Transect D in 1994. Among these regions four were clustered (all in 1994), three showed inhibition (i.e. the plankton patches were farther from fish shoals than would be expected from a random distribution of the patches around the shoals), and two were randomly distributed (Table 2).

The offshore region of Transect A in 1995 tended to have a significant horizontal overlap in both biomass and density (s_V) between acoustically-determined fish and zooplankton (Figure 7), as did the slope region of Transect D in 1995 (Figure 8). Generalized Additive models were significant ($p<0.1$) for offshore A2, A3, A5, D1, D2, and A4 (average within-patch s_V only). In 1994 the offshore region of Transect A showed a significant relationship between fish and plankton within-patch s_V only. These regions, with a significant fish–plankton overlap, mostly had intermediate levels of plankton. There was no consistent distance-based proximity pattern for these regions in 1995 (one was clustered, two showed inhibition, one was random and two showed clustering at smaller distances).

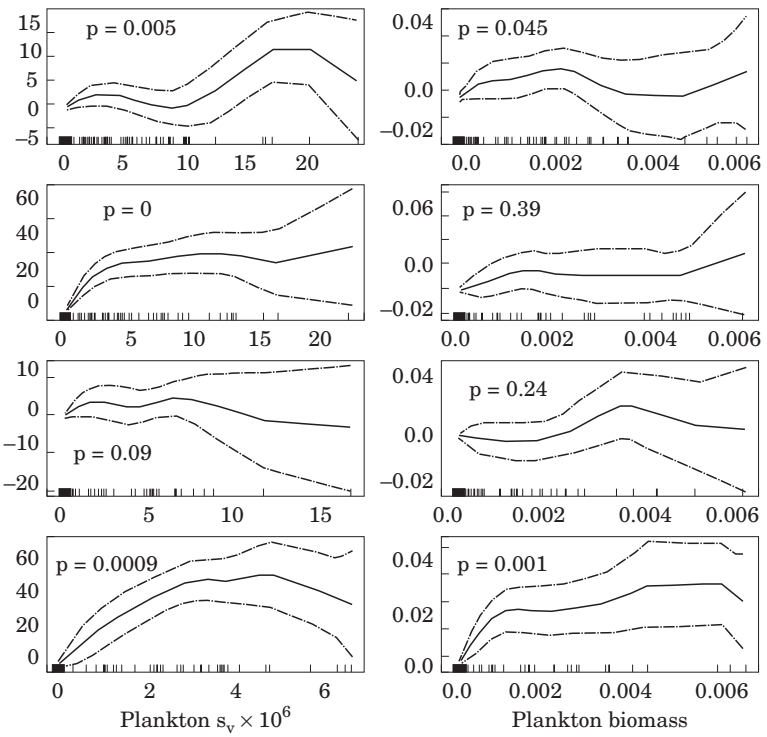

Figure 7. Results of Generalized Additive models regressions for transect A2-5 plankton s_V (left) and biomass (right) on fish s_V and biomass, respectively, for September 1995 offshore.

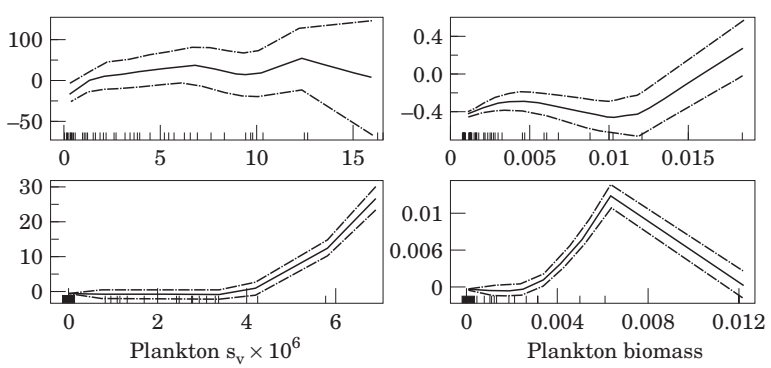

Figure 8. Transect D 1995 slope region Generalized Additive models for fish shoal s_V (left) and biomass (right) as a function of plankton patch s_V and biomass.

The frontal region of transect A in 1995 had low plankton biomass (0.004–0.020 km^{-1}) and medium to high fish biomass (0.107–0.76 km^{-1}), while in 1994 this region had higher plankton biomass (0.069–0.083 km^{-1}) and medium fish biomass (0.073–0.172 km^{-1}). The transect A runs having low plankton densities in the frontal region (<0.01 km^{-1}) for 1995 tended to have the distance-based proximity test indicate clustering of plankton patches around fish shoals (except A1), as did all 1994 runs for the transect A frontal region (with higher plankton biomass). Despite the apparent proximity of plankton patches to fish shoals in the transect A frontal region, there was no consistent evidence for a significant relationship between binned fish and plankton biomass from the GAM models (Table 2).

The offshore region of Transect A in 1995 had lower fish biomass (0.049–0.072 km^{-1}) than the frontal region, but higher plankton biomass (0.013–0.037 km^{-1}). The distance-based proximity tests in this region tended to indicate a random or inhibited

distribution of plankton patches around fish shoals (Table 2), but also tended to have a significant GAM test association between plankton and fish for both within-patch s_V and total biomass (6 of 10 tests were significant with $p<0.01$, the major exception again being A1). The offshore region of Transect A in 1994, with high fish densities (0.149–0.402 km^{-1}) and high plankton densities (0.072–0.134 km^{-1}), showed no consistent pattern of distance-based proximity, but had a significant GAM relationship between the average s_V of plankton and fish (Table 2). The GAM relationship in this region in 1995 for both average s_V and total biomass (for runs A2–A5) showed an increase in both s_V and total fish biomass with increasing plankton s_V and total biomass, respectively, for the lower range of plankton densities (Figure 7). Above some plankton threshold levels (s_V values of $2.5–5 \times 10^{-6}$; total biomass values between 0.005 and 0.01[3]), there was a decrease or levelling off in the s_V and total fish biomass with further increases in s_V and total plankton biomass.

Transect D offshore, with low plankton biomass in both years (except run D2 in 1995), showed strong evidence for clustering of plankton around fish, but no statistical evidence for spatial overlap in s_V or biomass between fish and plankton from the GAM model (Table 2). The transect D slope region, with generally higher plankton and fish biomass than offshore, had plankton randomly distributed around fish shoals (except D2 in 1995, which had very low plankton and fish biomass in the slope region and had the plankton clustered around the fish). In 1995, the transect D frontal region had a significant GAM relationship between fish and plankton s_V and biomass (Table 2 and Figure 8). The GAM relationship differed in the slope region between runs D1 and D2. Run D1 had a relationship similar to that found for the offshore region of transect A; increasing fish s_V and total fish biomass with increasing plankton s_V and total plankton biomass at low plankton s_V and biomass levels, but with no consistent pattern for higher plankton levels. Transect D2, with low plankton biomass (Figure 6), showed an increase in fish s_V with increasing plankton s_V at higher plankton s_V levels ($>4 \times 10^{-6}$; Figure 8). This may be a reflection of the low plankton levels in this region forcing fish to remain close to the higher plankton biomass patches (the 1995 D2 slope region had clustering of plankton patches around fish shoals) to have sufficient food, while the lower s_V levels ($1–3 \times 10^{-6}$ in Figure 8) were too low for sustained feeding.

Nearshore regions tended to have low biomass of fish and plankton and generally showed evidence for clustering of plankton patches around the fish shoals[4] (Figure 6, Table 2).

Evaluation of plankton identification algorithm

As our work is the first attempt at locating plankton patches using a two-frequency differencing method, along with morphological image processing, independent evaluation of the method was needed. We compared acoustic predictions with MOCNESS samples along Transect A during 1994 and 1995. We compared the depth distribution of acoustically-derived zooplankton biomass with concentrations of net-sampled euphausiids and the dominant copepod, *Calanus marshallae* (Figures 9 and 10). Data were not available for all regions both day and night, but there were sufficient data for a comparison. The net samples were not taken simultaneously with the acoustic transects, although they were within a day or two of all survey transect runs. The 1995 acoustic values used for comparison were the average of several runs, while for 1994, with only a single day and night run of each transect, we used the actual values for each run. The depths in these figures were the upper end of each 10 m range for the acoustic sample and the lower end of each (variable depth) range for the net samples.

Both the acoustic data and net samples showed plankton below the thermocline in the front and offshore during the daytime. The depth modes for the acoustic samples were generally within 10 m of the depth modes from the net samples. Results for offshore night net samples in 1995 are the average of two stations, while all the other net-sampled depth distributions are for a single net sample. The small net sample size and their time separation from the acoustic data suggests caution in interpreting these data.

Discussion

The results of plankton patch and fish shoal spatial distributions for 2 years and two transects both day and night over three front or depth-delineated regions combined with tests for distance-based proximity and spatial overlap strongly suggest that the spatial proximity of plankton and fish is influenced by the within-patch s_V and total plankton biomass. We hypothesize that there are two important thresholds for shoaling juvenile pollock feeding on zooplankton. The first is a plankton

[3]Notice that these values are biomass per 250 m bin, not per km as in Figure 6.

[4]Some confusion might arise from our looking at the distance-based proximity between fish and plankton from the viewpoint of the fish. We compute the proximity measure for each fish shoal and take the average of these. An observer might expect clustering of fish around plankton, rather than plankton around fish. However, since we interpret results in terms of fish we have chosen to look at the distribution of plankton patches around fish shoals.

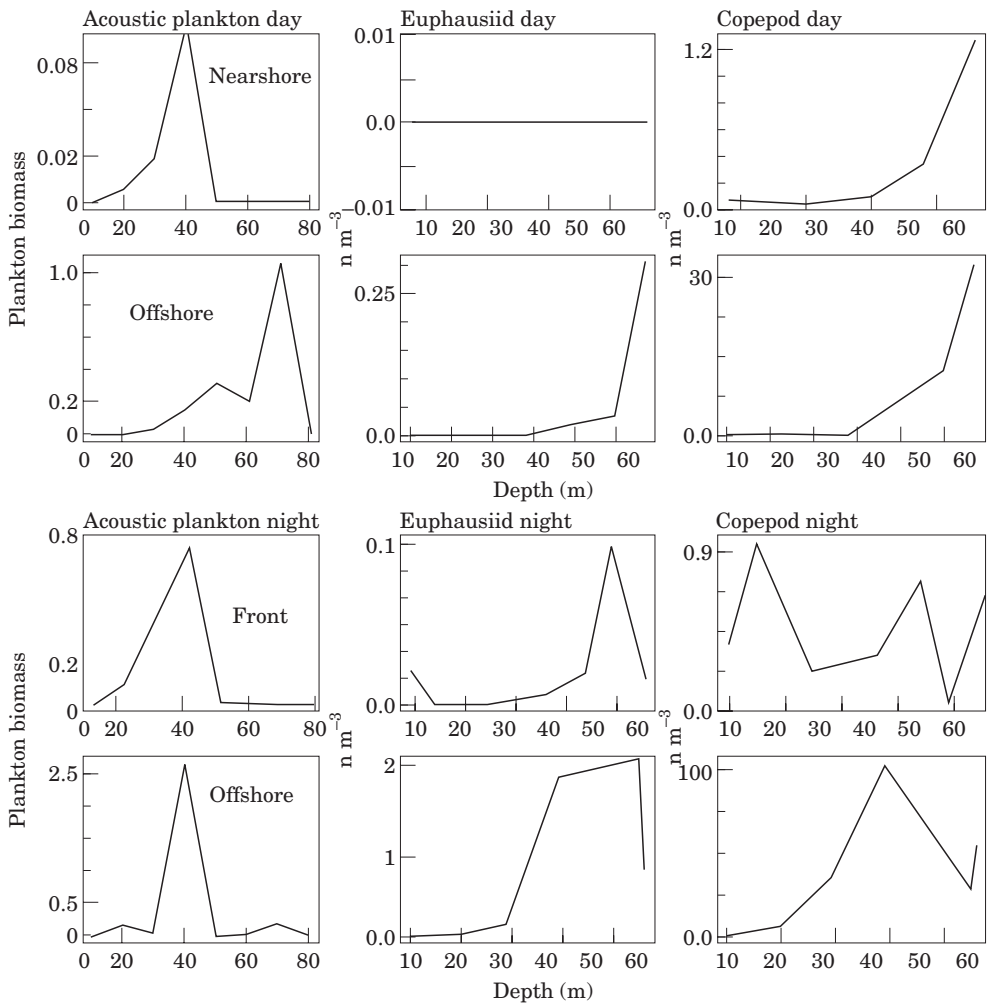

Figure 9. Transect A comparison of acoustically determined depth distribution of plankton, both day and night with MOCNESS net survey depths for euphausiids and copepods for 1994.

biomass density threshold below which, to achieve sufficient food to sustain growth, the fish may be required to remain close to their plankton prey (i.e. the plankton appear to be clustered around the fish in the distance-based proximity test; Figure 11a). The second threshold (for intermediate plankton biomass), is the within-patch plankton s_V level below which increasing plankton s_V is associated with increased within-shoal s_V. For many regions within this density range, the plankton-fish s_V association also applies to total biomass (i.e. increasing total plankton biomass below the second threshold is associated with higher fish total biomass; Figure 11b). Above this second within-patch s_V or total plankton biomass threshold, there is no apparent relationship between fish and plankton s_V or biomass (Figure 11c). The existence of this second threshold was supported by the data, which showed that when plankton biomass density was high, there was no consistent distance-based or GAM-elucidated proximity relationship between fish and plankton.

The magnitude of the proximity thresholds may influence the effect of prey distribution on fish growth, because they affect the amount of prey encountered by predators at different prey densities. Also, it may have an affect on other aspects of predator–prey dynamics, such as the amount of time spent searching and feeding. Modelling predator–prey dynamics between shoaling fish and patchy plankton has been limited by lack of information both on (a) the density of prey actually encountered by the feeding predator, in relation to the density sampled by net or other biomass samplers, and (b) the functional response of the predators to changing prey density (i.e. how does feeding rate change at different encountered prey densities). The ability to distinguish fish shoals from plankton patches acoustically and to place them in an explicit spatial relationship,

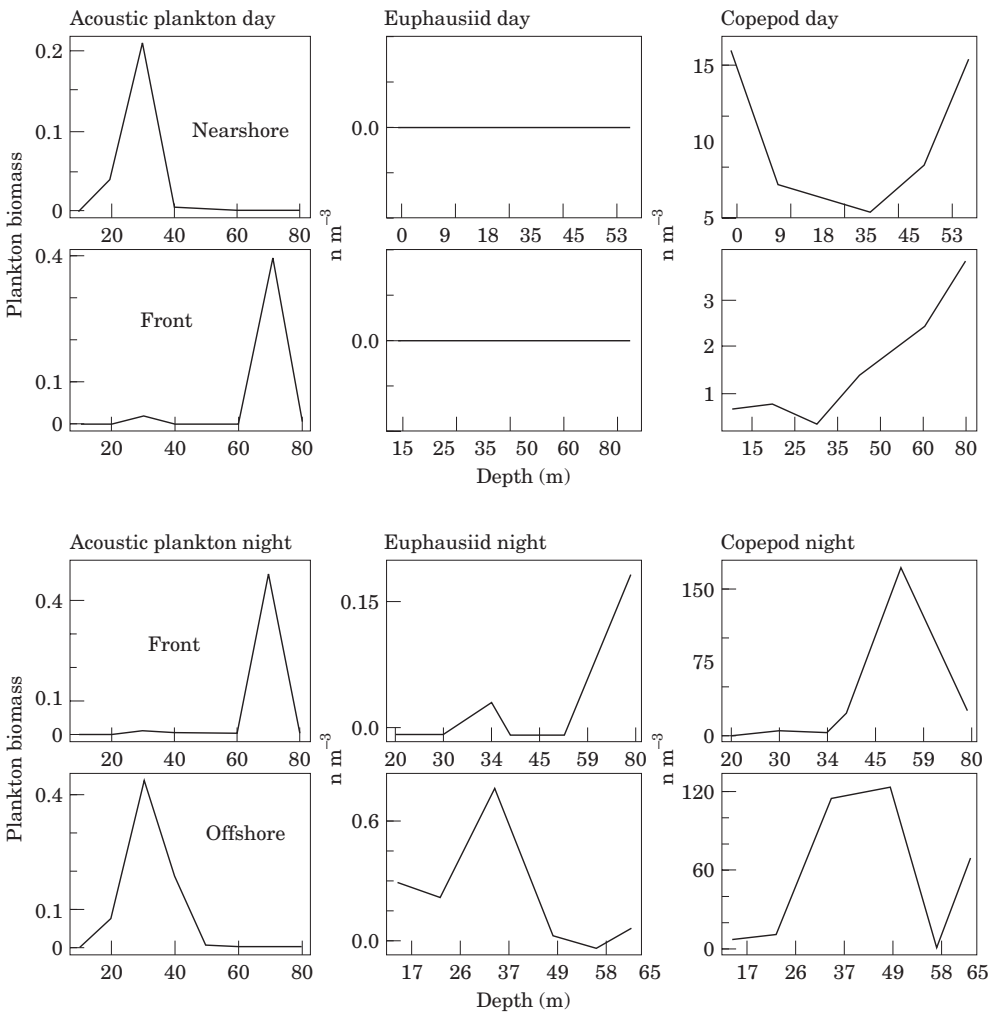

Figure 10. Transect A acoustically determined plankton depth distribution both day and night compared with MOCNESS net survey depths for euphausiids and copepods for 1995.

can provide guidance in both of these areas. The distribution of prey biomass at different distances from fish shoals (i.e. the distance-based proximity index) can be parlayed into an encounter rate, when fish swimming speed is used as a search rate. Similarly, the observed relationship between fish s_V (biomass) and plankton s_V (biomass) from the GAMs for intermediate plankton biomass density levels suggests a possible functional response for pollock feeding. The second threshold referred to above could be interpreted as the prey density level for maximum feeding rate and the first threshold could be interpreted as a prey level at which feeding rate has been reduced to half its maximum rate (i.e. the half-saturation prey level for feeding). In order to use these relationships for quantitative predictions, some assumption about the target strength of the fish and plankton would be needed to convert s_V to actual (not relative) biomass and numbers estimates. These can be obtained from net samples and geometric models or empirical determination (Stanton *et al.*, 1993; Traynor, 1996).

The monotonic association of fish and plankton s_V and biomass between the first and second threshold, and the levelling off or decline of fish s_V with increases in plankton s_V above the second threshold, is open to a variety of ecological interpretations. Either (1) in bins having higher within-patch s_V or total fish biomass the fish reduced the within-patch s_V or total plankton biomass through consumption; (2) there was sufficient food density above some threshold level such that fish were not attracted to finding higher density plankton patches; or (3) above the plankton s_V or biomass threshold, plankton more effectively avoided their predators.

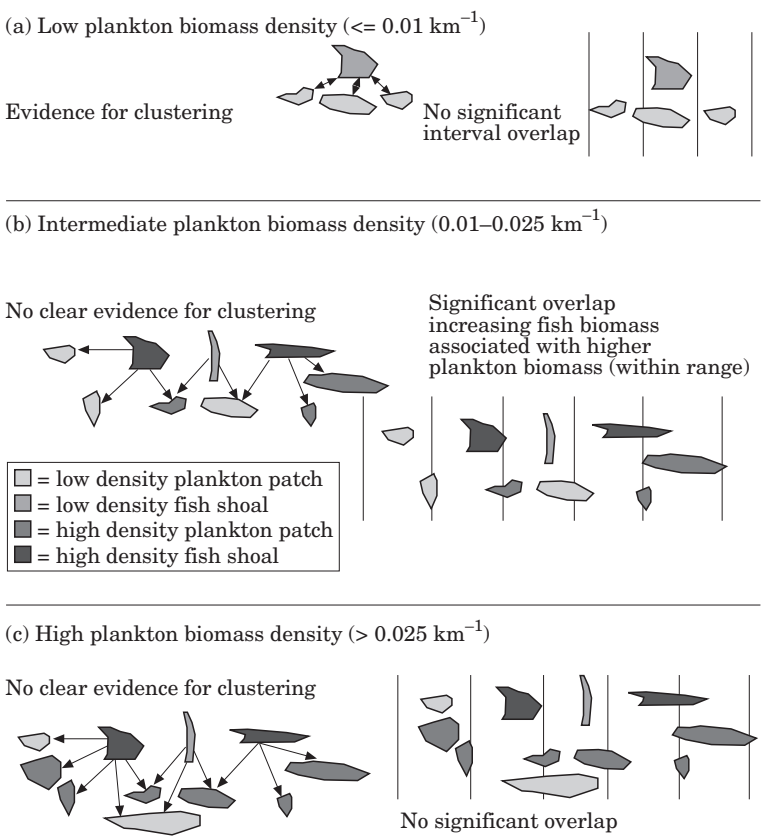

Figure 11. Pictograph showing the general changes in proximity between age-0 pollock shoals and plankton patches as plankton biomass density changes.

Examining the spatial association of biota at different trophic levels has been well suited to transect sampling and there are many examples of scale-related associations (Mackas and Boyd, 1979; Schneider and Piatt, 1986; Weber *et al.*, 1986; Coyle and Cooney, 1993; Horne and Schneider, 1997). Mackas *et al.* (1997) suggested an association between adult Pacific hake (*Merluccius productus*) and euphausiids off the coast of Vancounver Island. They used product-moment and rank order correlation between hake and euphausiids within 2 km horizontal bins and found values of 0.66 and 0.68, respectively. Echograms along two transects showed association between hake and euphausiids. However, the scale of the association is not known and correlation is not a strong measure of association. Fine-scale and non-correlation measures such as a distance-based proximity measure would strengthen the interpretation of predator–prey spatial associations. Rose and Leggett (1990) used spectral analysis to examine the spatial correlations (coherence) at different spatial scales between Atlantic cod (*Gadus morhua*) and capelin (*Mallotus villosus*). They found in-phase coherence (the same dominant frequency for both fish species) and positively correlated values between them at large scales (2–20 km) when the capelin did not have a thermal refuge, but only at very large scale (15–20 km) when the capelin were in temperatures above and below the preferred temperature range of cod. Spectral analysis allowed examination of spatial overlap at multiple bin sizes in a single computation, a distinct benefit. However, only correlation was examined and thus, monotonic relationships that were observed only over a range of density values (such as we found for fish and plankton in the intermediate plankton density regions) could not be detected (Star and Cullen, 1981).

Spatial association of patchy grey and predators is a relatively unexplored area. The results presented here and the hypotheses about overlap and distance-based proximity are, to our knowledge, new to the literature. Our results appear to indicate a stronger association between the s_V of fish and plankton than their biomass. With plankton patches and fish shoals that are often horizontally vast in extent, the fish may not be able to sense the prey patch biomass in choosing a feeding location, although some exploration of patch extent may possibly occur. It seems more likely that the within-patch density (s_V) is a more likely index of available food for a feeding fish than total biomass. Within-patch s_V is

a measure of the average biomass in a bin, which we used in our GAM model. Yet it is still unclear how the within-patch plankton s_V is linked to within-patch fish s_V (a within-shoal fish density measure). The observed relationship may imply that denser fish shoals are associated with denser plankton patches, while less dense shoals are near less dense plankton patches. However, the binning of biomass combines large and small patches, dense and diffuse patches into horizontal intervals, and makes biological interpretation of a significant association difficult.

Acoustic and net-identified plankton both showed strong evidence (Figures 9 and 10) for diel migration of zooplankton in the offshore region and, in 1994 in the frontal region as well. Juvenile pollock were largely restricted to the region above and up to the thermocline both day and night as verified in underwater videos taken in 1995 (Brodeur, 1998), although it is thought (Bailey, 1989) that larger juveniles begin migrating down through the thermocline during the daytime. Diel migration of pollock down through the thermocline has energetic advantages, because the lower temperatures reduce respiration (Ciannelli *et al*., 1998). Larger juvenile pollock (>50 mm) were found to feed largely during the night-time, presumably in surface waters, while smaller juveniles fed primarily during the day or during crepuscular periods (Brodeur *et al*., 1999). Although there was some acoustic evidence for fish below the thermocline (Figures 2 and 3), individual target strengths suggest that many of these are larger fish than juvenile pollock, and were probably age-1 and adult pollock (Lang *et al*., 1999). Except for nearshore environments, there was no acoustical or net sample evidence for zooplankton of sufficient size to be seen at our sampling frequencies being above the thermocline during the daytime in 1995, although in 1994, with a deeper thermocline, some plankton were sampled above the thermocline and acoustically-identified plankton were observed just above the thermocline. Since small pollock, inhabiting the thermocline region, were feeding primarily during the daytime and, since the diet of these fish was mostly copepods (Brodeur *et al*., 1999), these plankton in 1995 must have been either at too low a density or too small a size to be seen at 120 and 200 kHz or so closely associated spatially with the fish that their biomass was acoustically masked by backscatter from the fish. This conundrum could be partially resolved by more intensive plankton sampling and acoustic data collected at a higher frequency (e.g. 1 MHz or higher) in addition to the existing frequencies, where smaller plankton may be identified.

This paper emphasized the spatial association of fish shoals and their patchy plankton prey. The Pribilof Islands support large breeding colonies of northern fur seals and marine seabirds, several of which are piscivorous. The role of predation in influencing the spatial distribution of pollock was not considered here, but may be important. Pollock comprise the major prey in this region of several flatfish species and adult pollock (Lang *et al*., 1999), which tend to not be as abundant in this region as in other parts of the Bering Sea (Swartzman *et al*., 1994). Smaller juvenile pollock remained in the upper water column, reducing exposure to flatfish and adult pollock predation but leaving them exposed to piscivorous seabirds (Decker and Hunt, 1996). More study is needed on the role of predation on the spatial distribution of age-0 pollock, particularly in light of literature that suggests that biomass of many species may be top-down rather than bottom-up controlled (i.e. controlled by the abundance of predators rather than of prey; Springer, 1992; Verity and Smetecek, 1996). It may be that changes in growth from year-to-year affect the relative susceptibility of age-0 pollock to fish and other predators.

Optimal foraging theory, one of the major paradigms in predator–prey dynamics, suggests that a predator will stay within a prey patch as long as the density of prey within the patch is higher than the average density of prey in all patches (Charnov, 1976). The positive increase of pollock with increasing zooplankton density below the second threshold density, for intermediate levels of plankton biomass density, suggests that pollock may have been choosing higher density patches. We are cautious in this statement because horizontal overlap of predator and prey within bins does not demonstrate either feeding or vertical overlap. In addition, other factors (e.g. predator avoidance, energetics) may also have major effects on animal distribution.

We are intrigued with the suggested existence of biomass density thresholds governing choice of feeding by juvenile pollock. How common are such thresholds in feeding or in fact do they exist at all? Are they species or region specific? Do they change, depending on changing prey density conditions in the overall environment (as suggested by optimal foraging) or are the options coded within the species. Juvenile fish of many species (e.g. smelt, herring, alewife) are obligate shoalers and feed on diel-migrating plankton. As such, the proximity relationships suggested by this study may exist in many areas, particularly in shelf slope regions that often serve as juvenile nursing areas because of their high productivity. Studies in such juvenile rearing areas, with multifrequency acoustics, along with net sampling and environmental sampling can assess the generality of proximity and feeding options for this critical period of life. Whether such thresholds exist in the case of piscivorous fish is less clear, although these fish often eat plankton as well. We expect that many piscivorous fish spend significant time searching for prey, such that proximity between predators and prey may be more difficult to demonstrate at small spatial scales than for the planktivorous fish in this study. However, clustering of piscivorous fish around their prey may be more

prevalent than with the planktivorous juveniles of this study because prey densities will rarely be as high as the patch densities for plankton we encountered.

We have presented methods for distinguishing fish and plankton that rely on data at three frequencies. However, the availability of these frequencies is not prevalent, and many research vessels work with a single frequency or with two frequencies (38 and 120 kHz). Several researchers (Madureira *et al*., 1993; Mitson *et al*., 1996; Miyashita *et al*., 1997) have used 38 and 120 kHz data to distinguish fish from euphausiids. Madureira *et al*. (1993) found that zooplankton showed generally higher backscatter at the higher frequency while fish (capelin) did not. Since the bins used by Madureira *et al*. (1993) were averages of many pings, the method benefited from the law of averages over the large scale. However, it lacked the spatially explicit feature inherent in the morphological filter which is a strength of our methods. In regions where acoustic backscatter is dominated by two groups or sizes of scatterers, a two-frequency method may be adequate to distinguish juvenile fish and zooplankton, though testing of such an algorithm, by simultaneous net and acoustic sampling, is needed before the methods can be generally applied. Not only the depth distributions of the plankton net surveys, but also the expected backscatter from the net samples should be compared with acoustic backscatter (i.e. the forward problem; Wiebe *et al*., 1997).

We have examined the relative biomass and spatial distribution of pollock and plankton over several years, several transects, and several runs of the same transect both by day and night. Thus, we have addressed both spatial and temporal variability in the distribution patterns of these biota over a critical period in the life of Bering Sea pollock. We believe that feeding success enabling the rapid growth needed to escape predation plays a major role in pollock survival and hence year-class strength. However compelling this hypothesis is, we are still restricted to a small part of the life cycle of these fish and have covered only a part of their nursery area. The conditions observed over the study period may be the result of several alternative histories between which we cannot distinguish. For example, low pollock biomass around the Pribilof Islands may be due to poor feeding conditions resulting in high predation mortality, or to variable transport conditions that advected fewer larvae to this region. Further study of larval transport and energetic modelling of pollock growth and feeding may help distinguish between these alternatives. Energetics modelling can also be used to examine the impact of pollock on their plankton prey.

Acknowledgements

This paper is sponsored by the NOAA Coastal Ocean Program through the Southeast Bering Sea Carrying Capacity and is contribution S335. The authors would like to thank Phyllis Stabeno and Sigrid Salo for providing hydrographic information, Lorenzo Ciannelli and Robert Schabetsberger for helpful comments.

References

Bailey, K. M. 1989. Interaction between the vertical distribution of juvenile walleye pollock *Theragra chalcogramma* in the eastern Bearing Sea, and cannibalism. Marine Ecology Progress Series, 53: 205–213.

Brodeur, R. D. 1998. In situ observations of the association between juvenile fishes and scyphomedusae in the Bering Sea. Marine Ecology Progress Series, 163: 11–20.

Brodeur, R. D., and Wilson, M. T. 1996. Mesoscale acoustic patterns of juvenile walleye pollock (*Theragra chalcogramma*) in the western Gulf of Alaska. Canadian Journal of Fisheries and Aquatic Sciences, 54: 1953–1965.

Brodeur, R. D., Wilson, M. T., and Ciannelli, L. 1999. Spatial and temporal variability in feeding and condition of age-0 walleye pollock in frontal regions of the Bering Sea. ICES Journal of Marine Science, In press.

Brodeur, R. D., Wilson, M. T., Napp, J. M., Stabeno, P. J., and Salo, S. 1997. Distribution of juvenile pollock relative to frontal structure near the Pribilof Islands. Alaska Sea Grant AK-SG-97-01, pp. 573–589.

Charnov, E. 1976. Optimal foraging, the marginal value theorem. Theoretical Population Biology, 9: 129–136.

Ciannelli, L., Brodeur, R. D., and Buckley, T. W. 1998. Development and application of a bioenergetics model for juvenile walleye pollock. Journal of Fish Biology, 52: 879–898.

Coyle, K. O., and Cooney, R. T. 1993. Water column scattering and hydrography around the Pribilof Islands, Bering Sea. Continental Shelf Research, 13: 803–827.

Coyle, K. O., Hunt, G. L., Jr, Decker, M. B., and Weingartner, T. J. 1992. Murre foraging, epibenthic sound scattering, and tidal advection over a shoal near St George Island, Bering Sea. Marine Ecology Progress Series, 83: 1–14.

Decker, M. B., and Hunt, G. L., Jr 1996. Murre foraging at the frontal system surrounding the Pribilof Islands, Alaska. Marine Ecology Progress Series, 139: 1–10.

Diggle, P. J. 1983. Statistical analysis of spatial point patterns. Academic Press, London. 148 pp.

Foote, K., Knutsen, H., Vestnes, G., MacLennan, D., and Simmonds, J. 1987. Calibration of acoustic instruments for fish density estimation: a practical guide. Cooperative Research Report, International Council for the Exploration of the Sea, No. 144. 57 pp.

Haralick, R., and Shapiro, L. 1992. Computer and Robot Vision. Vol 1. Addison-Wesley, Reading, Mass. 672 pp.

Hastie, T., and Tibshirani, R. 1990. Generalized Additive Models. Chapman and Hall, London.

Holliday, D. V., and Pieper, R. E. 1995. Bioacoustical oceanography at high frequencies. ICES Journal of Marine Science, 52: 279–296.

Horne, J. K., and Schneider, D. C. 1997. Spatial variance of mobile aquatic organisms: capelin and cod in Newfoundland coastal waters. Philosophical Transactions of the Royal Society of London Series B, 352: 633–642.

Lang, G. M., Brodeur, R. D., Napp, J. M., and Schabetsberger, R. 1999. Variation in groundfish predation on juvenile walleye pollock relative to hydrographic structure near the Pribilof Islands, Alaska. ICES Journal of Marine Science, In press.

Mackas, D. L., and Boyd, C. M. 1979. Spectral analysis of zooplankton spatial heterogeneity. Science, 204: 62–64.

Mackas, D. L., Kieser, R., Saunders, M., Yelland, D. R., Brown, R. M., and Moore, D. F. 1997. Aggregation of euphausiids and Pacific hake (*Merluccius productus*) along the outer continental shelf off Vancouver Island. Canadian Journal of Fisheries and Aquatic Sciences, 54: 129–136.

Madureira, L. S. P., Ward, P., and Atkinson, A. 1993. Differences in back-scattering strength determined at 120 kHz and 38 kHz for three species of Antarctic macrozooplankton. Marine Ecology Progress Series, 93: 17–24.

Mitson, R. B., Simard, Y., and Goss, C. 1996. Use of a two-frequency algorithm to determine size and abundance of plankton in three widely spaced locations. ICES Journal of Marine Science, 53: 209–215.

Miyashita, K., Aoki, I., Seno, K., Taki, K., and Ogishima, T. 1997. Acoustic identification of isada krill, *Euphausia pacifica* Hansen, off the Sanriku coast, north-eastern Japan. Fisheries Oceanography, 6: 266–271.

Nero, R. W., and Magnuson, J. J. 1989. Characterization of patches along transects using high-resolution 70-kHz integrated acoustic data. Canadian Journal of Fisheries and Aquatic Sciences, 46: 2055–2064.

Rose, G. A., and Leggett, W. C. 1990. The importance of scale to predator–prey spatial correlations: an example of Atlantic fishes. Ecology, 71: 33–43.

Schneider, D. C., and Piatt, J. F. 1986. Scale-dependent correlation of seabirds with schooling fish in a coastal ecosystem. Marine Ecology Progress Series, 32: 237–246.

Springer, A. M. 1992. A review: walleye pollock in the North Pacific – how much difference do they really make? Fisheries Oceanography, 1: 80–96.

Stabeno, P. J., Schumacher, J. D., Salo, S. A., Hunt, G. L., and Flint, M. 1998. The physical environment around the Pribilof Islands. *In* The Bering Sea: Physical, Chemical and Biological Dynamics. Ed. by T. R. Loughlin and K. Ohtani. Alaska Sea Grant Press.

Stanton, T. K., Chu, D., Wiebe, P. H., and Clay, C. S. 1993. Average echoes from randomly oriented random-length finite cylinders: Zooplankton models. Journal of the Acoustic Society of America, 94: 3463–3472.

Star, J. L., and Cullen, J. J. 1981. Spectral analysis: a caveat. Deep Sea Research, 28: 93–97.

Swartzman, G., Stuetzle, W., Kulman, K., and Wen, N. 1994. Modeling the distribution of fish schools in the Bering Sea: Morphological school identification. Natural Resource Modeling, 8: 177–194.

Swartzman, G., Brodeur, R., Napp, J., Walsh, D., Hewitt, R., Demer, D., Hunt, G., and Logerwell, E. 1999. Relating spatial distributions of acoustically determined patches of fish and plankton: Image Analysis, Data Viewing and Spatial Proximity. Canadian Journal of Fisheries and Aquatic Sciences, In press.

Traynor, J. J. 1996. Target-strength measurements of walleye pollock (*Theragra chalcogramma*) and Pacific whiting (*Merluccius productus*). ICES Journal of Marine Science, 53: 253–258.

Urick, R. J. 1983. Principles of Underwater Sound. McGraw-Hill, New York. 423 pp.

Verity, P. G., and Smetacek, V. 1996. Organisms life cycles, predation, and the structure of marine pelagic ecosystems. Marine Ecology Progress Series, 130: 277–293.

Weber, L. H., El-Sayed, S. Z., and Hampton, I. 1986. The variance spectra of phytoplankton, krill and water temperature in the Antarctic Ocean south of Africa. Deep Sea Research, 33: 1327–1343.

Wiebe, P. H., Burt, K. H., Boyd, S. H., and Morton, A. W. 1976. A multiple opening/closing net and environmental sensing system for sampling zooplankton. Journal of Marine Research, 34: 313–326.

Wiebe, P. H., Stanton, T. K., Benfield, M. C., Mountain, D. G., and Greene, C. H. 1997. High-frequency acoustic volume backscattering in the Georges Bank coastal region and its interpretation using scattering models. IEEE Journal of Oceanic Engineering, 22: 445–464.